Microchimica Acta (2018) 185: 551
https://doi.org/10.1007/s00604-018-3083-0

ORIGINAL PAPER

An electrochemical chlorpyrifos aptasensor based on the use of a glassy carbon electrode modified with an electropolymerized aptamer-imprinted polymer and gold nanorods

Mahmoud Roushani[1] · Azizollah Nezhadali[2] · Zeynab Jalilian[2]

Received: 12 July 2018 / Accepted: 5 November 2018 / Published online: 15 November 2018

Abstract

A highly selective and sensitive aptasensor is described for voltammetric determination of the pesticide chlorpyrifos (CPS). The sensor was constructed by modifying a glassy carbon electrode (GCE) with gold nanorods and a polymer that was molecularly imprinted with an aptamer against CPS. This results in double specific recognition. Under optimal conditions and a working potential as low as 0.22 V (vs. Ag/AgCl), the nanotools has a dynamic range that covers the 1.0 fM - 0.4 pM CPS concentration range, and the detection limit is 0.35 fM. This is lower than any of the previously reported methods. This MIP-aptasensor is selective over structural analogs, stable, and adequately reproducible. It was successfully applied to the determination of CPS in spiked food samples.

Keywords o-Dihydroxybenzene · o-Phenylenediamine · Hexacyanoferrate · Nanohybrid · Differential pulse voltammetry · Electrochemical impedance spectroscopy · Pesticide

Introduction

Chlorpyrifos is one of the many organophosphate pesticides (OPPs). According to previous reports, exposure to chlorpyrifos (CPS) can lead to change of polyamine metabolism and induce oxidative stress and can also cause DNA damage [1]. Chlorpyrifos is considered extremely toxic because when it enters food, it has detrimental effect on humans and animals [2]. Therefore, monitoring the behavior of CPS residues is important for human health. Significant efforts have been devoted to developing direct techniques for the determination of pesticides [3–10] Among these methods, electrochemical aptasensors play an important role and this is due to their high sensitivity, excellent specificity, convenience, easily detectable signals and simplicity; thus, decreasing the analysis time and cost [11].

Aptamers are synthetic single-stranded functional DNA or RNA molecules which are selected from random oligonucleotide libraries by an in vitro evolution process named SELEX (systemati evolution of ligands by exponential enrichment) [12]. Aptamers were replaced by antibodies as diagnostic elements in bioavailability because of the ease of producing, more stability, easy labeling and lower cost. Due to these, aptamer-based assay were established using various detection methods [13–15]. Among these methods, electrochemical aptasensors play an important role for their excellent specificity, high sensitivity, easily detectable signals, and simplicity and is easily modified for their detection and immobilization by the introduction of reporter molecules and functional groups [16, 17].

Metal nanoparticles with different nanostructures including rings, spheres, rods and cages have been used in various applications [18–22]. Among them, the subtle behavior of gold nanorods (AuNR) revealed that they have the ability to promote faster electron transfer and distinct optical properties depended on their shape and thus, electron transfer between electrode and analytes reactions in electrochemical reactions [22]. Therefore, to further enhance the amount of effective

Electronic supplementary material The online version of this article (https://doi.org/10.1007/s00604-018-3083-0) contains supplementary material, which is available to authorized users.

✉ Mahmoud Roushani
mahmoudroushani@yahoo.com; m.roushani@mail.ilam.ac.ir

[1] Department of Chemistry, Ilam University, PO. Box 69315-516, Ilam, Iran

[2] Department of Chemistry, Payame Noor University, PO. Box19395-4697, Tehran, Iran

binding sites in the assay and supply larger electrochemically active surface areas, the aptasensor was decorated with nanoparticles such as AuNR [23].

Molecularly imprinted polymer receptors (MIPs), as novel materials and biomimetic molecular recognition elements have been widely applied in various fields [24–26]; this is due to the presence of such unique properties as desired selectivity, superb physical and chemical stability, commercial availability as well as low cost, compared to those of enzymes, antibodies and receptors [27]. Usually, typical MIPs include template molecules, functional monomers, cross-linking reagents; which nowadays, MIP films are most commonly polymerized by sol-gels, bulk polymerization and precipitation polymerization. Behind the polymerization, the template molecules are removed from the final polymer matrixes [28–30]. These methods often have limitations such as partial template removal, slow mass transfer and rebinding kinetics in sensor applications [31]. Therefore, the electrochemical polymerization was suggested because it is one of the efficient ways of solving these limitations by generating a rigid, uniformed compact MIP film with controlled thickness onto the work electrode surface of any shape and size [32, 33].

The aim of this study was to develop a highly sensitive electrochemical aptasensor based on electro polymerized MIP and AuNR for the determination of CPS. The exploitation of gold nanorods improved the electron transfer rate and provided a high surface area for immobilization of the MIP-aptamer. The fabricated MIP-aptasensor shows excellent selectivity, sensitivity, as well as satisfactory results for the detection of CPS in real samples.

Experimental

Materials and reagents

The amino modified aptamer against CPS was purchased from Bioneer Co, (South Korea, http://www.bioneer.com). The sequence of nucleotides in the aptamer is shown below; the sequence contained 91 bases. (5′-NH_2 modified) (5′-CCTG CCACGCTCCGCAAGCTTAGGGTTACGCCTGCAGC GATTCTTGATCGCGCTGCTGGTAATCCTTCTTTAAG CTTGGCACCCGCATCGT-3′). They had been HPLC-purified and freeze-dried by the supplier and was kept for further use. Cetyltrimethyl ammonium bromide (CTAB), Sodium borohydride ($NaBH_4$), Tetra chloroauric acid ($HAuCl_4$), Silver nitrate ($AgNO_3$), o-Dihydroxybenzene (o-DB), o-phenylenediamine (o-PD) and CPS were received from Sigma–Aldrich Co. (https://www.sigmaaldrich.com), LLC (USA) (www.usa-corporate.com) or Merck (www.merck.com) companies.

Apparatus

All electrochemical experimental data including differential pulse voltammetry (DPV), electrochemical impedance spectroscopy (EIS), and cyclic voltammetry (CV) data, were carry out with μ-AUTOLAB electrochemical system type III and FRA2 board computer controlled Potentiostat/Galvanostat (Eco-Chemie, Switzerland) driven with NOVA software in conjunction with a conventional three electrode system and in 5 mM $Fe(CN)_6^{3-/4-}$ solution. The working electrode was a modified GCE, and the auxiliary and reference electrodes were a platinum wire and an Ag/AgCl (satd 3.0 M KCl), respectively. The impedance analysis was performed in a frequency range between 0.1 Hz and 100 kHz with a modulation voltage of 5 mV. Cyclic voltammetry measurements were taken from −0.2 to 0.7 V as initial and stop potential. The DPV measurements were carried out by scanning the potential of −0.2 to 0.7 V with modulation time of 50 ms and modulation amplitude of 25 mV. Scanning electron microscopy (SEM) images were obtained by using FESEM apparatus (Model: Hitachi S4160). Transmission electron microscopy (TEM) image was recorded by a Hitachi H-800 electron microscope. The absorption measurement was investigated using an ultraviolet-visible (UV–Vis) spectrophotometer (VARIAN 300Bio CARY) in dual beam mode with a 1 cm quartz cuvette.

Synthesis of the gold nanorods (AuNR)

The AuNR was synthesized by making reference to reported methods in previous literatures and by making some modifications to them [20]. This section is presented in Electronic Supplementary Material.

Preparation of aptamer-MIP

The aptamer-MIP was synthesized by referring to the reported methods in previous literatures [34, 35]. Aptamer-MIP solution was prepared in the following procedure: first, 0.1 mM CPS was added to 0.05 M phosphate buffer (pH = 7.6) containing 1 μM of the aptamer to form the CPS–aptamer complex and stirred for 5 min. Then, 0.01 g of o-Dihydroxybenzene (o-DB) and 0.01 g of o-phenylenediamine (o-PD) were dissolved in 6 mL of 0.05 M Tris-HCl buffer (pH = 8.0) and afterwards 4 mL of the CPS–aptamer complex (prepared above) was added and mixed for 5 min. Subsequently, non-imprinted polymer (NIP) modified electrode were prepared analogous to the MIP without adding CPS (template).

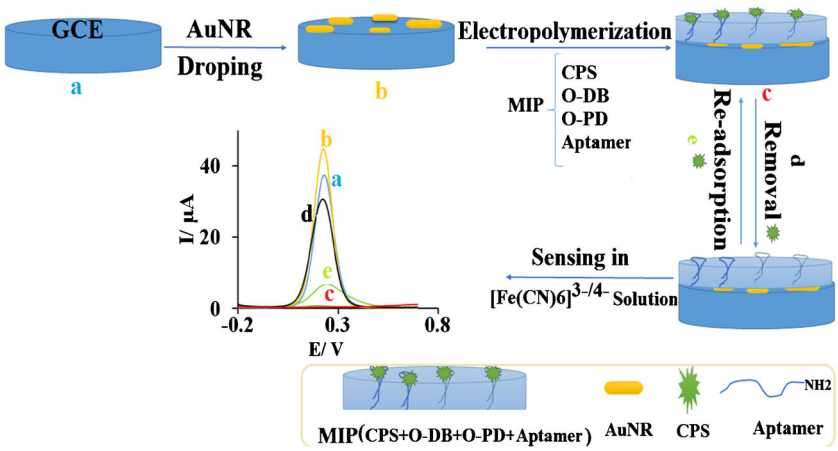

Scheme 1 Schematic representation of electrochemical MIP-aptasensing assay for CPS detection

Fabrication of MIP-aptasensor

The fabrication process for the electrochemical aptasensor is shown in Scheme 1 and the procedure is described thus: the GCE was polished carefully with alumina powder (0.05 μm) on a soft polishing cloth; and then rinsed thoroughly with ultrapure distilled water and dried before use. Thereafter, 10 μL of synthesized AuNR solution was dropped onto the surface of the freshly polished GCE and dried at room temperature. In the following, the obtained AuNR/GCE was immersed in a solution containing polymerization solution (aptamer-MIP prepared in section preparation of aptamer-MIP). By applying a potential range between 0 to 1.0 V for 10 cycles, with scan rate of 50 mVs^{-1}, the aptamer-MIP was electropolymerized on the AuNR/GCE surface and the aptamer-MIP/AuNP/GCE as the aptasensor was achieved. Then, the washing solution containing methanol–nitric acid (4:1, *v*/v) was used to remove the CPS molecules from the cavities and holes in the MIP on the modified electrode surface. The aptamer-NIP/AuNP/GCE was fabricated by the same method, but without the CPS template.

Sample preparation

Food samples including apples and lettuce purchased from the supermarket were washed, dried, chopped into 3 × 3 mm particles approximately. 10 g of each sample was sprayed with different concentrations of chlorpyrifos. After equilibration for 3 h at room temperature to make pesticide absorbed into the samples, 10 mL mixed solution of acetone and 0.1 M pH 7.5 phosphate buffer (1/9, *v*/v) was added to the above samples.. Then the suspension was separated from the insoluble materials by centrifugation for 20 min at 1008 rcf and finally, it was filtered to remove the large particles [36]. The residue was diluted with water and detects the advance assay by standard addition method.

Results and discussion

Choice of materials

Ortho-phenylenediamine (o-PD) and o-dihydroxybenzene (o-DB) was chosen as functional monomer because of several reasons. First, after electropolymerization, the skeleton of MIP film can form groups such as –NH and –OH, these groups can more effective imprinted site [34]. Second, the o-PD layer appears to confer selectivity by limiting access of large molecules to the surface. Thus, biochemicals larger than o-PD cannot penetrate the film. For this reason, we chose to use o-PD to make selective CPS assay. Also, the amino group and benzene ring can provide recognition sites through hydrogen bonds and "π-π stacking" interaction with analyzing CPS. The o-PD proved to be easily electropolymerized on various substrate materials and form films with good chemical and mechanical stability. O-Dihydroxybenzene have been used as electron transfer mediators in electrochemical processes due to their high electron transfer efficiency, excellent redox reversibility and low cost. AuNR based platforms can provide more stable biosensing systems due to their rods-like shapes compared to nanoparticles. Besides, the modification of the electrodes using AuNR can facilitate a higher conductive surface by providing an enhanced electron transfer, and thus they offer the enhanced modified electrode response with in a high sensitivity. Compared with similarly sized spherical nanoparticles, AuNR exhibit higher absorption cross section in near-infrared (NIR) frequencies. The characteristic surface plasmon band of colloidal gold nanoparticles is observed in the visible range; however, AuNR have a surface plasmon band in the near-infrared region with a coexisting weaker band in the visible region. Moreover, the experimental protocols used in the synthesis of AuNR allow tuning their surface plasmon resonance into the biological window of the electromagnetic spectrum [37–42]. The designed nanotools based of aptamer-MIP [PmDB-PoPD] and AuNR had many advantages, such as good mechanical and chemical stability,

low–cost, high sensitivity, excellent selectivity, simple, and possibility of in–situ testing.

Characterization of synthesized gold nanorods

This section is presented in Electronic Supplementary Material.

Characterization of the modified electrode

To evaluate the morphologies and surface of the different modified electrodes, the SEM technique was used. Fig. 1 shows the SEM images of the bare GC (A), AuNR/GC (B) and aptamer-MIP/AuNR/GC electrodes. After the AuNR on the surface of the bare electrode which shows the uniform surface was immobilized (Fig. 1a), the structures of the rod corresponding to AuNR (Fig. 1b) can be clearly observed. In the next step, after electro polymerization, the complex MIP and aptamer and the formation of the aptamer-MIP film on the surface of AuNR/GCE (Fig. 1c), the surface morphology was changed and became uneven and rough. The results also showed that MIP linked to the surface of AuNR further expands the surface area on the modified electrode for more recognition of CPS. It was speculated that the AuNR possibly form N-Au bonding with the inner surface of o-PD molecules, which in turn results in the dense layer of NIP multilayer nanofilms, in the absence of CPS molecule (Fig. 1d).

Electrochemical characterization of the designed MIP-aptasensor

EIS is a favored technique to investigate the surface features of the modified electrodes at each immobilization step. According to this technique, the information was obtained about the charge transfer resistance (R_{ct}). Fig. 2a shows the Nyquist plots of impedance spectroscopy of bare GCE (a), AuNR/GCE (b), MIP-aptamer/AuNR/GCE before (c) and after (d) extraction of CPS and modified GCE after immersing in 0.1 pM CPS solution (e) in anion redox probe solution ($Fe(CN)_6^{3-/4-}$). From the results, it can be observed that black curve (Fig. 2a, curve a) shows a small semicircle (R_{ct} = 406.0 Ω), which was a characteristic feature of the diffusion controlled electrochemical processes. With the addition of the 10 μL of AuNR to the surface, GCE bear (Fig. 2a, curve b) obviously reduced the resistance of the redox probe (R_{ct} = 186.0 Ω), for a better electric conducting performance of AuNR. In the next stage, by electropolymerization of the PoDB/PoPD and the CPS–aptamer complex onto the AuNR/GCE surface, increase in the semi-circular diameter (R_{ct} = 18.07 KΩ) revealed that the aptamer-MIP film impeded the transfer of electrons and reduced the electron transfer rate (Fig. 2a, curve c). This can be due to the interaction between the $–NH_2$ group of Apt and AuNR. Afterwards, the resistance of the modified electrode decreased with the removal of CPS from the MIP (Fig. 2a, curve d); but since the CPS molecule can matched with MIP cavity, it was enhanced again with the re-adsorption of CPS onto the MIP (Fig. 2a, curve e).

Apart from the ESI technique, the fabricated MIP-aptasensor which was used to validate the immobilization of

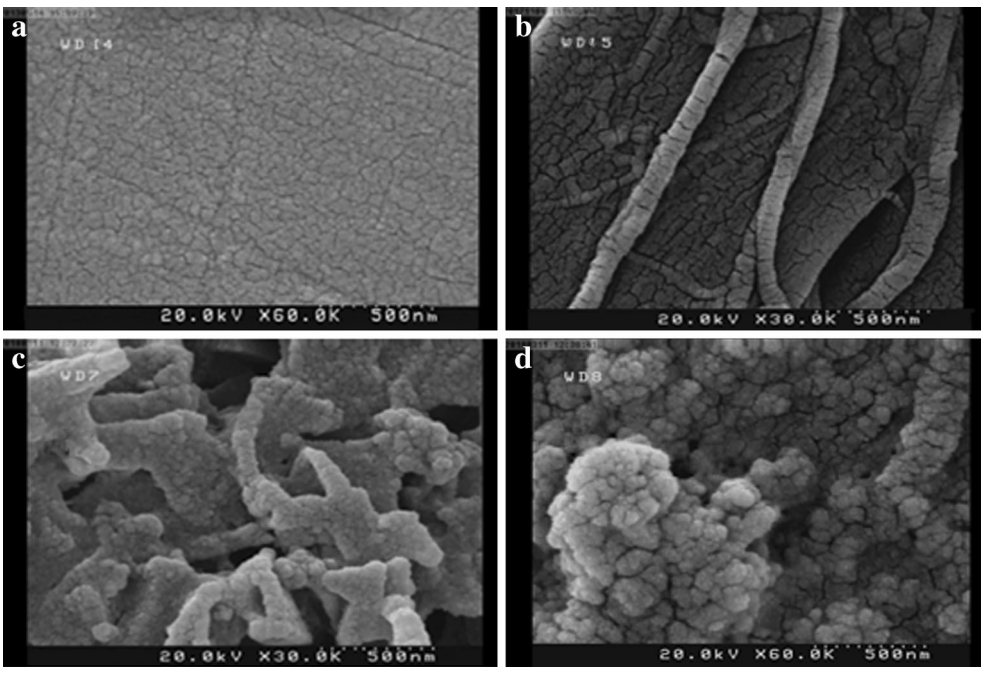

Fig. 1 SEM images related to bare GCE (A), AuNR/GCE (B) and MIP-aptamer/AuNR/GCE (C) and NIP-aptamer/AuNR/GCE (D)

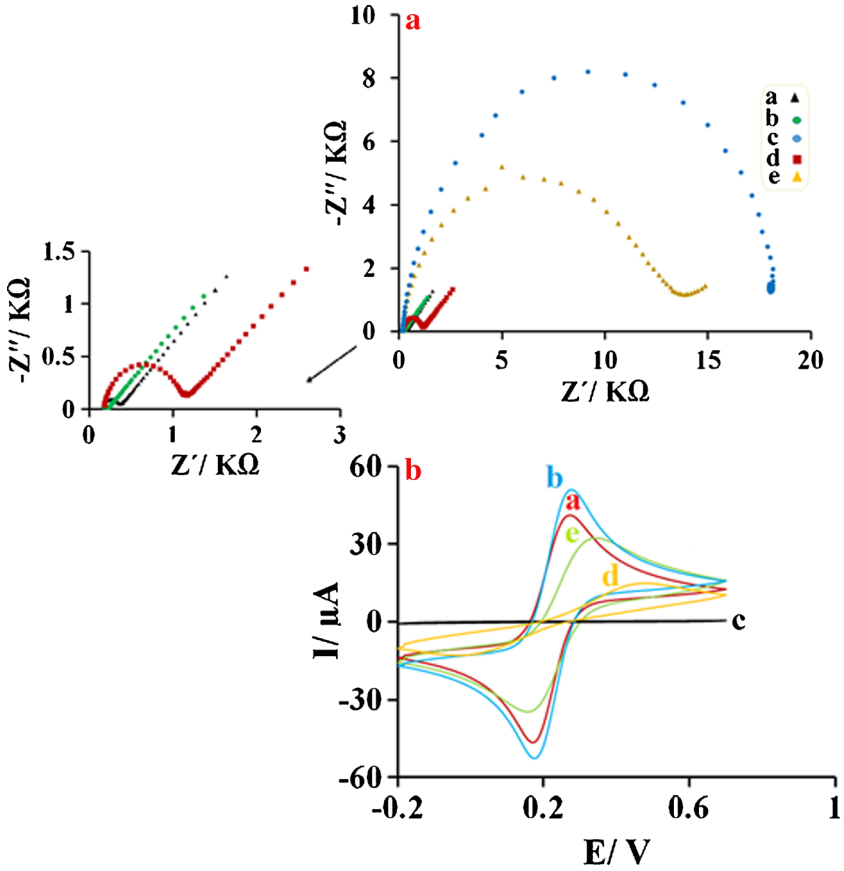

Fig. 2 (A) Nyquist curves and (B) CVs of 5 mM $[Fe(CN)6]^{3-/4-}$ in 0.5 mM KCl recorded for bare GCE (a), AuNR/GCE (b), aptamer-MIP/AuNR/GCE before (c) and after (d) extraction of CPS and aptamer-MIP/AuNR/GCE after immersing in 0.1 pM CPS solution (e). The EIS was performed in a frequency range between 0.1 Hz and 100 kHz with a modulation voltage of 5 mV

the substrates in each step was characterized by cyclic voltammetry in 5 mM Fe $(CN)_6^{3-/4-}$solution. Fig. 2b indicates the cyclic voltammograms of the different steps of modification processes. The CVs displayed the bare GCE (Fig. 2b, curve a). When the AuNR was pipetted on the bare GCE surface, a height current appeared which was attributed to the significant enhancement of the effective surface area of the electrode in the presence of AuNR resulting in facilitating the electron-transfer rate. In the following, a very small current illustrating the successful electropolymerization of the immobilized PoDB/PoPD and the CPS–aptamer complex onto the surface of the AuNR/GCE indicated that the level was completely blocked. However, after the removal of CPS from the MIP, the blockade receded, and the current response was enhanced again (Fig. 2b, curve d). In the next stage, the MIP-aptasensor was once more immersed in the 0.1 pM CPS solution and the blockade was strengthened again. This led to the current decrease in the redox via the CPS adsorbed to the copolymer. The results above are in accordance with the characterization by ESI.

Molecular imprinted electropolymerization

In order to confirm the process of electropolymerization MIP-aptasensor on the surface of AuNR/GC electrode, this parameter was investigated by recording of related CV. As shown in Fig. S2 that the PoDB/PoPD and the CPS–aptamer complex were formed via gradually depositing the non-conducting film onto the AuNR/GCE surface with an increasing number of CV scans. Formation the PoDB/PoPD and the CPS–aptamer complex onto the AuNR/GCE surface obstruct the electron transfer from/to the redox probe $[Fe(CN)_6]^{3-/4-}$. Presence the sharp oxidation peak and equable oxidation peak

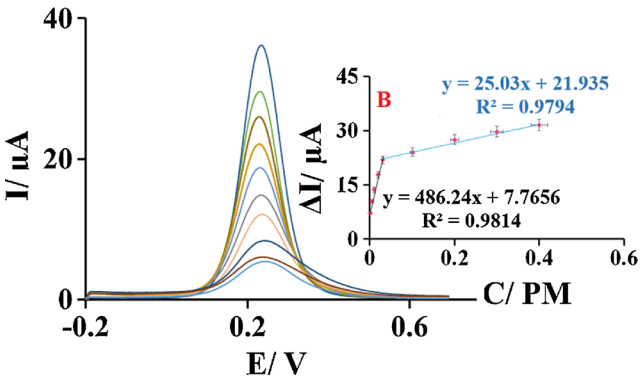

Fig. 3 (A) DPV responses of the aptasensor in 5 mM $[Fe(CN)_6]^{3-/4-}$ after incubation with 0.001, 0.005, 0.01, 0.02, 0.05, 0.1, 0.2, 0.3, and 0.4 pM of CPS. Inset is the calibration plot of peak current vs. CPS concentration The DPV measurements are performed from −0.2 to 0.7 V, with incubation time 9 min, amplitude of 50 mV and a pulse width of 50 ms.

Table 1 Comparison of analytical methods for the detection of CPS

Method	Modified Electrode	LOD (nM)	Linear Range (nM)	Ref.
Cyclic voltammetry	Apt/Fc@WMCNTs/OMC/GCE	0.33	$1000–10^8$	[36]
Differential puls voltammetry	Apt/AMP/CuO NFs SWCNTs/Nafion/GCE	0.07	0.1–150	[43]
Cyclic voltammetry	Apt/GO@Fe_3O_4/CB/GCE	0.033	$0.1–10^5$	[44]
Chemiluminescence	–	0.92	0.001–2.0	[45]
Differential puls voltammetry	AuNPs-CSs modified BDD	1.29×10^{-4}	0.01–100	[46]
Square Wave Voltammetry	C_3N_4 NTs@GQD/GCE	0.001	0.01–1.00	[47]
Differential puls voltammetry	MIP-aptamer/AuNR/GCE	0.35×10^{-6}	1×10^{-6}– 400×10^{-6}	This work

in the potential of 0.43 V and 0.7 V, respectively, show the oxidation peak might be assigned to the easily oxidative amine group and hydroxyl group of the monomers and electrochemical polymerization of o-PD and o-DB was irreversible. Finally, in the potential range of 0–1.0 V, the chemical structure doesn't change with the process of electropolymerization.

Optimization of method

To obtain excellent analytical efficiency of the prepared MIP-aptasensor, optimization of the elution time and incubation time parameters was done by the CV method. Respective data and Figures are given in the Electronic Supporting Material Thus, 25 min was chosen as the optimal time for CPS removal (Fig. S3) and 9 min was chosen as the optimal time for incubation of CPS (Fig. S4) and applied to all further experiments.

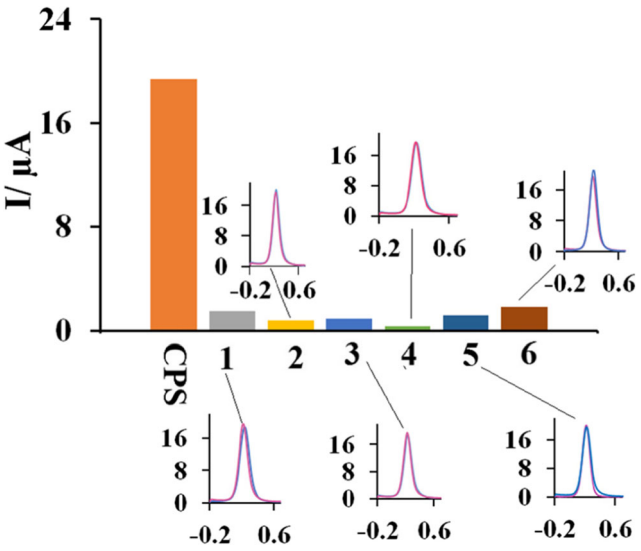

Fig. 4 Histogram of the DPV response change related to the designed nanotools after being incubated with pesticides compound: 1) Asulam, 2) Aflatoxin-B1, 3) Dimethoat, 4) Acetamiprid, 5) Carbofuran, 6) Malathion (100 nM) and CPS (1 pM)

Analytical performance of the MIP-aptasensors

Under optimal working conditions (desorption time: 25 min and incubation time: 9 min), the MIP-aptasensor was used for the sensitive detection of CPS. Fig. 3a displays the DPV calibration plot of the designed aptasensor using 9 different CPS (0.001 to 0.4 pM) standards in 5 mM $[Fe(CN)_6]^{3-/4-}$ solution. The results from these analyses demonstrated that the DPV response of the aptasensor diminished with enhancement of the CPS concentration and gave two linear ranges from 0.001–0.03 pM and 0.03–0.4 pM. Furthermore, the linear regression fit was $\Delta I\ (\mu A) = 486.24\ [CPS]\ (pM) + 7.76$ ($R^2 = 0.98$) and $\Delta I\ (\mu A) = 25.03\ [CPS\ (pM) + 21.935$ ($R^2 = 0.98$). The detection limit (LOD) based on $S/N = 3$ was calculated to be 0.35 fM and the value of the LOD is lower than that of other reported methods in the literature (Table 1).

Selectivity, reproducibility and stability of the aptasensor

The selectivity of molecularly imprinted aptasensor was investigated by interferents which included structurally similar molecules and similar property with CPS by higher concentrations than that of CPS. This case was studied by identifying the current response, when the aptasensor was immersed in the 100.0 nM of each interfering substance such as Asulam, Aflatoxin-B1, Dimethoat, Acetamiprid, Carbofuran and Malathion. The results are illustrated in Fig. 4.

Table 2 The resultant data for CPS detection in real samples with this electrochemical nanotool ($n = 4$)

Sample	Added CPS (fM)	Found CPS (fM)	RSD%	Recovery%
apples	20	19.53	2.7	97.65
	100	102.56	3.1	102.5
	200	198.34	2.9	99.1
Lettuce	20	19.64	3.2	98.2
	100	103.2	3.8	103.2
	200	203.8	3.3	101.9

Also, the reproducibility of the prepared aptasensor was evaluated with the use of five aptasensors into a 5 mM $[Fe(CN)_6]^{3-/4-}$ solution. All the modified electrodes exhibited similar electrochemical responses and the RSD = 3.1%, indicating a good reproducibility of the explained strategy.

The repeatability of the designed strategy was estimated into a 5 mM $[Fe(CN)_6]^{3-/4-}$ solution by analyzing a certain amount of CPS by five aptasensors, for 18 days. It was observed that about 97.9% and 92.3% of the initial response of the nanotool for CPS remained after being stored at 4 °C for 5 days and 18 days, respectively. The obtained data illustrated the relatively high repeatability of this electrochemical nanotool.

Analysis of real samples

The analytical effectiveness of this strategy for the real quantification of CPS was assayed through the analysis of fruit and vegetable samples. The determinations were performed using a standard addition method and analyzed using independently prepared aptasensors. As shown in Table 2, the determined values were in good agreement with the added pesticide concentrations and indicated the excellent reliability the biosensor for the detection of CPS in real samples.

The promising results obtained with aptamer/MIP-based electrochemical assay for the detection of analyte in complex matrices have some advantages such as low cost, easy preparation, high sensitivity and higher selectivity and stability.

Conclusions

In summary, in the present study, a double recognition method for the ultra-selective detection of CPS is reported. Interest of this strategy is combination of aptasensing and molecular imprinting strategies for designing a highly sensitive system to overcome some of the faced challenge by other methods. The AuNR excellent characteristics as sensing interface make this nanoparticle as an attractive matrix for covalently aptamer-MIP immobilization. By following removal of CPS, the double recognition imprinting cavities were formed, indicating recognition properties superior to that of aptamer or traditional molecularly imprinting alone. The analytical usefulness of this nanotool was finally demonstrated by analyzing the real samples. Overlay, it can be easily extended and it has the potential to be applied for detecting other pesticide in food and environmental samples.

Compliance with ethical standards The author(s) declare that they have no competing interests.

References

1. Chen D, Jiao Y, Jia H, Guo Y, Sun X, Wang X, Xu J (2015) Acetylcholinesterase biosensor for chlorpyrifos detection based on multi-walled carbon nanotubes-SnO_2-chitosan nanocomposite modified screen-printed electrode. Int J Electrochem Sci 10: 10491–10501
2. Talan A, Mishra A, Eremin SA, Narang J, Kumar A, Gandhi S (2018) Ultrasensitive electrochemical immuno-sensing platform based on gold nanoparticles triggering chlorpyrifos detection in fruits and vegetables. Biosens Bioelectron 105:14–21
3. Lin GF, Wang YH, Li GC, Bai W, Zhang H, Wang SC (2014) Construction and application of molecularly imprinted film sensor on determination of chlorpyrifos in water. Adv Mater Res 936:843–849
4. Sun X, Gao C, Zhang L, Yan M, Yu J, Ge S (2017) Photoelectrochemical sensor based on molecularly imprinted film modified hierarchical branched titanium dioxide nanorods for chlorpyrifos detection. Sensors Actuators B Chem 251:1–8
5. Uygun ZO, Dilgin Y (2013) A novel impedimetric sensor based on molecularly imprinted polypyrrole modified pencil graphite electrode for trace level determination of chlorpyrifos. Sensors Actuators B Chem 188:78–84
6. Szpyrka E, Matyaszek A, Slowik-Borowiec M (2017) Dissipation of chlorantraniliprole, chlorpyrifos-methyl and indoxacarb-insecticides used to control codling moth (Cydia Pomonella L.) and leafrollers (Tortricidae) in apples for production of baby food. Sci Pollut Res 24(13):12128–12135
7. Seddik H, Z Marstani Z, ALazzam T (2017) Trace level determination of insecticide using gas chromatography, and the application for residual monitoring in local Syrian vegetables. Arab J Chem 10: 212–218
8. Xiao Z, He M, Chen B, Hu B (2016) Polydimethylsiloxane/metal-organic frameworks coated stir bar sorptive extraction coupled to gas chromatography-flame photometric detection for the determination of organophosphorus pesticides in environmental water samples. Talanta 156–157:126–133
9. Walton I, Davis M, Munro L, Catalano VJ, Cragg PJ, Huggins MT et al (2012) A fluorescent dipyrrinone oxime for the detection of pesticides and other organophosphates. Org Lett 14(11):2686–2689
10. Shim JY, Kim YA, Lee EH, Lee YT, Lee HS (2008) Development of enzyme-linked immunosorbent assays for the organosphorus insecticide EPN. J Agric Food Chem 56(24):11551–11559
11. Shahdost-fard F, Roushani M (2017) Designing an ultra-sensitive aptasensor based on an AgNPs/thiol-GQD nanocomposite for TNT detection at femtomolar levels using the electrochemical oxidation of Rutin as a redox probe. Biosens Bioelectron 87:724–731
12. Basnar B, Elnathan R, Willner L (2006) Following aptamer-thrombin binding by force measurements. Anal Chem 78(11): 3638–3642
13. Fang L, Lu Z, Wei H, Wang E (2008) A electrochemiluminescence aptasensor for detection of thrombin incorporating the capture aptamer labeled with gold nanoparticles immobilized onto the thio-silanized ITO electrode. Anal Chim Acta 628(1):80–86
14. Nagatoishi S, Tanaka Y, Tsumoto K (2007) Circular dichroism spectra demonstrate formation of the thrombin-binding DNA aptamer G-quadruplex under stabilizing-cation-deficient conditions. Biochem Biophys Res Commun 352(3):812–817
15. Lu Y, Li X, Zhang L, Yu P, Su L, Mao L (2008) Aptamer-based electrochemical sensors with aptamer-complementary DNA oligonucleotides as a probe. Anal Chem 80(6):1883–1890
16. Shahdost-fard F, Roushani M (2017) The use of a signal amplification strategy for the fabrication of a TNT impedimetric nanoaptasensor based on electrodeposited NiONPs immobilized onto a GCE surface. Sensors Actuators B Chem 246:848–853

17. Ghanbari K, Roushani M (2018) A nanohybrid probe based on double recognition of an aptamer MIP grafted onto a MWCNTs-chit nanocomposite for sensing hepatitis C virus core antigen. Sensors Actuators B Chem 258:1066–1071
18. Langille MR, Personick ML, Zhang J, Mirkin CA (2012) Defining rules for the shape evolution of gold nanoparticles. J Am Chem Soc 134(35):14542–14554
19. Jana NR, Gearheart L, Murphy CJ (2001) Wet chemical synthesis of high aspect ratio cylindrical gold nanorods. J Phys Chem B 105(19):4065–4067
20. Nikoobakht B, El-Sayed MA (2003) Preparation and growth mechanism of gold nanorods (NRs) using seed-mediated growth method. Chem Mater 15(10):1957–1962
21. Jana NR (2005) Gram-scale synthesis of soluble, near-monodisperse gold nanorods and other anisotropic nanoparticles. Small 1(8–9):875–882
22. Perez-Juste J, Pastoriza-Santos I, Liz-Marzan LM, Mulvaney P (2005) Gold nanorods: synthesis, characterization and applications. Coord. Chem Rev 249(17–18):1870–1901
23. Shu Y, Chen J, Xu Q, Wei Z, Liu F, Lu R, Xu S, Hu X (2017) MoS_2 nanosheet–au nanorod hybrids for highly sensitive amperometric detection of H_2O_2 in living cells. J Mater Chem B 5:1446–1453
24. Yang G, Zhao F (2015) Electrochemical sensor for dimetridazole based on novel gold nanoparticles@molecularly imprinted polymer. Sensors Actuators B Chem 220:1017–1022
25. Wang Sh SG, Chen Z, Liang Y, Zhou Q, Pan Y, Zhai H (2018) Constructing a novel composite of molecularly imprinted polymer-coated AuNPs electrochemical sensor for the determination of 3-nitrotyrosine. Electrochim Acta 259:893–902
26. Riskin M, Ran TV, Bourenko T, Granot E, Willner I (2008) Imprinting of molecular recognition sites through electropolymerization of functionalized au nanoparticles: development of an electrochemical TNT sensor on π-donor-acceptor interactions. J Am Chem Soc 130(30):9726–9733
27. daSilva H, Pacheco JG, MCSMagalhães J, Viswanathan S, Cristina Delerue-Matos C (2014) MIP-graphene-modified glassy carbon electrode for the determination of trimethoprim. Biosens Bioelectron 52:56–61
28. Ensafi AA, Amini M, Rezaei B (2018) Molecularly imprinted electrochemical aptasensor for the attomolar detection of bisphenol a. Microchim Acta 185:265
29. Malitesta C, Mazzotta E, Picca RA, Poma A, Chianella I, Piletsky SA (2012) MIP sensors- the electrochemical approach. Anal Bioanal Chem 402(5):1827–1846
30. Aghaei A, Milani Hosseini MR, Najafi M (2010) A novel capacitive biosensor for cholesterol assay that uses an electropolymerized molecularly imprinted polymer. Electrochim Acta 55(5):1503–1508
31. Gholivand MB, Karimian N (2015) Fabrication of a highly selective and sensitive voltammetric ganciclovir sensor based on electropolymerized molecularly imprinted polymer and gold nanoparticles on multiwall carbon nanotubes/glassy carbon electrode. Sensors Actuators B Chem 215:471–479
32. Lian W, Liu S, Yu J, Xing X, Li J, Cui M, Huang J (2012) Electrochemical sensor based on gold nanoparticles fabricated molecularly imprinted polymer film at chitosan–platinum nanoparticles/grapheme gold nanoparticles double nanocomposites modified electrode for detection of erythromycin. Biosens Bioelectron 38:163–169
33. Liu YT, Deng J, Xiao XL, Ding L, Yuan YL, Li H, Li XT, Yan XN, Wang LL (2011) Electrochemical sensor based on a poly(Para-aminobenzoic acid) film modified glassy carbon electrode for the determination of melamine in milk. Electrochim Acta 56:4595–4602
34. Zhao X, Liu Y, Zuo J, Zhang J, Zhu L, Zhang J (2017) Rapid and sensitive determination of tartrazine using a molecularly imprinted copolymer modified carbon electrode (MIP-PmDB/PoPD-GCE). J Electroanal Chem 785:90–95
35. Li S, Liu C, Yin G, Qun Zhang Q, Luo J, Wu N (2017) Aptamer-molecularly imprinted sensor base on electrogenerated chemiluminescence energy transfer for detection of lincomycin. Biosens Bioelectron 91:687–691
36. Jiao Y, Jia H, Guo Y, Zhang H, Wang Z, Sun X, Zhao J (2016) An ultrasensitive ptasensor for chlopyrifos based on ordered mesoporous carbon/ferrocene hybrid a multiwalled carbon nanotubes. RSC Adv 6(63):58541–58548
37. Wen W, Huang JY, Bao T, Zhou J, Xia HX, Zhang XH, Wang SF, Zhao YD (2016) Increased electrocatalyzed performance through hairpin oligonucleotide aptamer-functionalized gold nanorods labels and graphene-streptavidin nanomatrix: highly selective and sensitive electrochemical biosensor of carcinoembryonic antigen. Biosens Bioelectron 83:142–148
38. Narang J, Malhotra N, Singh G, Pundir CS (2015) Electrochemical impediometric detection of anti-HIV drug taking gold nanorods as a sensing interface. Biosens Bioelectron 66:332–337
39. Arvand M, Gholizadeh TM (2013) Gold nanorods–graphene oxide nanocomposite incorporated carbonnanotube paste modified glassy carbon electrode for voltammetric determination of indomethacin. Sensors Actuators B Chem 186:622–632
40. Murphy CJ, Sau TK, Gole AM, Orendorff CJ, Gao J, Gou L, Hunyadi SE, Li T (2005) Anisotropic metal nanoparticles: synthesis, assembly, and optical applications. J Phys Chem B 109:13857–13870
41. Chakraborty S, Joshi P, Shanker V, Ansari ZA, Singh SP, Chakrabarti P (2011) Contrasting effect of gold nanoparticles and nanorods with different surface modifications on the structure and activity of bovine serum albumin. Langmuir 27:7722–7731
42. Pissuwan D, Valenzuela SM, Cortie MB (2008) Prospects for gold nanorod particles in diagnostic and therapeutic applications. Biotechnol Genet Eng Rev 25:93–112
43. Jiao Y, Houa W, Fua J, Guoa Y, Suna X, Wanga X, Zhaoa J (2017) A nanostructured electrochemical aptasensor for highly sensitive detection of chlorpyrifos. Sensors Actuators B Chem 243:1164–1170
44. Chen S, Chen X, Xia T, Ma Q (2016) A novel electrochemiluminescence sensor for the detection of nitroaniline based on the nitrogen-doped graphene quantum dots. Biosens Bioelectron 85:903–908
45. Xie C, Li H, Li S, Gao S (2011) Surface molecular imprinting for chemiluminescence detection of the organophosphate pesticide chlorpyrifos. Microchim Acta 174:311–320
46. Wei M, Zeng G, Lu Q (2014) Determination of organophosphate pesticides using an acetylcholinesterase-based biosensor based on a boron-doped diamond electrode modified with gold nanoparticles and carbon spheres. Microchim Acta 181:121–127
47. Lütfi Yola M, Atar N (2017) A highly efficient nanomaterial with molecular imprinting polymer: carbon nitride nanotubes decorated with graphene quantum dots for sensitive electrochemical determination of chlorpyrifos. J Electrochem Soc 164(6):B223–B229